An Experimental Investigation of the Flutter Characteristics of Low Density Wings

by

John J. Deyst, Jr.

MASS. INST. OF TECHNOLOGY
JUL 1958
LIBRARY

Submitted in Partial Fulfillment
of the Requirements for the
Degree of Bachelor of Science
at the
MASSACHUSETTS INSTITUTE OF TECHNOLOGY

June, 1958

Signature redacted

Signature of Author . . . .
Department of Aeronautical Engineering

Signature redacted

Certified by . . . .
Thesis Supervisor

Accepted by . . . .
Chairman, Departmental Committee on Theses

AN EXPERIMENTAL INVESTIGATION OF THE FLUTTER CHARACTERISTICS OF LOW DENSITY WINGS, by JOHN J. DEYST, Jr.

ABSTRACT

Flutter calculations for wings of low density have proven to be of little value in the past due to the inconservative estimates yielded by the analyses. There has arisen some doubt as to the validity of the usual assumptions made in doing this kind of work, particularly the aerodynamic assumptions that lead to the predictions of the forces acting on the wing. This thesis is an attempt to investigate the flutter characteristics of this type of wing and validate or disprove the analytical methods of analysis. The results obtained definitely uphold the aerodynamic theories and assumptions used in analysis of these wings.

Thesis Supervisor: Holt Ashley, Sc. D.

Title: Associate Professor of Aeronautical Engineering.

LIST OF SYMBOLS

Symbol	Definition
a	Distance between the elastic axis and the midchord point divided by one half of the chord length; positive if the elastic axis is aft of the midchord.
A	Cross-sectional area.
b	One half of the chord length (feet).
d	Distance from the elastic axis to the point of cantilever of the leaf springs.
EI	Flexural rigidity.
g	Damping coefficient.
h	Vertical coordinate of the elastic axis measured from the neutral position.
I_α	Mass moment of inertia per unit span about the elastic axis.
K	Spring constant.
L	Lift.
ℓ	Spring length.
m	Mass per unit span.
M	Moment.
$\mathcal{M}$	Total mass.
Q	Generalized force.
r_α	Dimensionless radius of gyration.
s	Wing span
S	Projected wing area (square feet).
S_α	Static mass moment per unit span about the elastic axis (positive when the center of gravity is aft).
T	Instantaneous kinetic energy of the system.
U	Instantaneous potential energy of the system.

LIST OF SYMBOLS (cont.)

Symbol	Definition
U_∞	Free stream velocity
X_α	Dimensionless static unbalance.
x	Coordinate along the spring length measured from the point of attachment to the wing.
y	Spanwise coordinate.
z	Vertical coordinate.
α	Angle of attack.
ρ	Density.
ω	Frequency.
∂	Mathmatical operator (partial differentiation).
μ	Density ratio.

SUBSCRIPTS

cs	Coil spring.
LS	Leaf spring.
S	Spring.
i	Identification of a particular degree of freedom (Lagrange's equation).
D	Divergence.

TABLE OF CONTENTS

I

INTRODUCTION

A number of experimental investigations have been carried out by the (NACA), and others, attempting to determine the cause of inconservative predicted, flutter speeds determined by theoretical analyses of wings of low density; inconservative in this case meaning the theoretically predicted flutter speed exceeds the actual flutter speed of the wing. Theory predicts that, for any particular wing configuration, the dimensionless flutter speed becomes infinite as the density ratio approaches zero (all other parameters held constant). The theory predicts that the flutter speed, as a function of density will suddenly increase at a particular density ratio as this density ratio is approached from higher density ratios, and the plot of the relationship will become asymptotic to a particular line of constant density ratio. All of the investigations mentioned above, except one done in water*, indicate a discrepency in the theory. There were no tendencies for the flutter speed to increase and as a matter of fact the opposite tendency was often the case in these investigations. Due to the conflicting results it was decided to experimentally and analytically investigate

*Reference #5

the phenomonon and attempt primarily to uphold or disprove the validity of the aerodynamic portion of the analysis.

The most basic type of flutter analysis done is the "typical section analysis." This method involves the simplest aerodynamic solution. Because this is the most fundamental analytical problem it eliminates many of the assumptions that enter into analyses of three dimensional wings. We have therefore, a minimum of engineering approximations if we are analysing a two dimensional flow experiment.

During the planning and actual construction of the experimental model two goals were always kept to the fore. First the model was built as light as possible, without sacrificing the required strength, and second it was built to as close a physical approximation as was possible, of the "ideal" model used in "typical section" analysis*. The experimental model used in this thesis was essentially an elastically supported rigid body, mounted to produce two dimensional flow over its surfaces. It had two degrees of freedom, bending and torsion and possessed a specific elastic axis perpendicular to the direction of airflow.

*Reference to Fig. #2

II

THE EXPERIMENT

Description of the Experimental Model

The experimental model was a rigid, constant section,* wing segment mounted elastically . It was built almost entirely of balsa wood sheet and strips and covered with silkspan. The construction was made as light as possible.

The model was provided with a steel tube mounted through its own center of gravity and lying in the chord plane of the wing. The tube stretched between the end ribs and was mounted parallel to the leading and trailing edges. The tube could be filled with lead weights to increase the effective density of the wing or, could itself be removed in order to obtain a minimum density ratio of ($\mu = 1.56$). This minimum μ being well below the theoretical asymptote of infinite flutter speed. Thus a number of density ratio's varying between the minimum and a maximum of ($\mu = 6.24$) could be obtained. In this way an entire density range across the asymptote was investigated.

Two large vertical fairings were built into the throat of the M. I. T. Student Wind Tunnel, which served both to maintain two dimensional flow and also to mount the wing. These fairings stretched for eight feet along the direction

*N.A.C.A. (23-009)

of the flow and thus were approximately four times the length of the wing chord. The wing was mounted between these fairings with a minimum of clearance between the wing and the fairings.

The wing was restrained by three sets of springs. There were two sets of cantilevered leaf springs and one set of coil springs. The coil springs were mounted at what became the elastic axis of the system and were attached at top and bottom to the fairings. These provided only translational restraint to the wing. The leaf springs which, for analytical purposes were uniform steel beams, were cantilevered into the wing end ribs and pin jointed fore and aft into the fairings. They were mounted into the end ribs close to the leading and trailing edges and extended ahead and behind the wing respectively. These leaf springs contributed both bending and torsional restraint to the system. The reason for this method of spring restraint was for obtaining frequency ratios of well below one. This made the system comparitively insensitive to changes in this ratio and conversely made the analysis of the system less sensitive to errors in measurement of this ratio.

In order to allow the model to translate and rotate it was necessary to cut comparitively large holes in the fairings to permit the leaf springs to deflect. This of course disturbed the two dimensional flow pattern. As a remedy, tip plates were mounted at the extreme ends of the wings in vertical positions such that they covered, to a good extent, the aforementioned holes. These were large enough to cover the holes under all conditions of translation and rotation of the wing.

The close tolerances between fairing and wing end plate were a cause of difficulty in that they represented a good percentage of the damping encountered in the experiment. The clearances were however, kept to a minimum (approximately $\frac{1}{16}''$) which helped to maintain two dimensional flow.

In order to excite the wing while running a flutter test a long chord was tied to one of the springs where it was mounted into the wing end rib. The chord lead out of the tunnel enabling the experimenter to excite the wing at will during a test.

Above all else the wing construction and accompanying hardware were made as light as possible. The wing itself was specifically designed and constructed to investigate the asymptotic flutter velocities as the density ratio was reduced.

Model Parameters and Methods of Obtaining Them

The model was run at six density ratios. All pertinent flutter parameters except a and x_α , varied with the density ratio. The methods for obtaining these parameters were partly experimental and partly analytical. All parameters which could not be directly measured were analytically calculated from measurable quantities.

At each density ratio a measurement of natural torsional frequency about the elastic axis was taken. The wing was restrained by pinning its elastic axis to the fairing, thus allowing rotation about but no translation of the elastic axis. Strain gages mounted on one of the leaf springs and connected to a Sanborn recorder made it possible to get a good measurement of the frequency when the wing was deflected and released. From this and an analytical analysis of the leaf springs yielding K_α, I_α and r_α were obtained for each density ratio. The natural translational frequency could not be readily measured because the wing could not be restrained to translational motion only. The spring constants of the coil springs were measured experimentally and along with the translational restraint of the leaf springs which was again calculated analytically, a value for K_h was obtained. With the mass of the wing this yielded ω_h. Thus we could calculate ω_h/ω_α.

The effective mass of the wing was not measurable directly and therefore had to be analytically determined. This effect is due to the fact that the spring restraints are not massless and their masses partially contribute to the effective mass and therefore the effective density ratio of the wing. In this thesis μ always refers to this effective density ratio. The methods for calculating this effect are explained in Appendix I.

The damping coefficient g was also an extremely difficult quantity to measure. The estimation of this quantity is taken up later in the section on the theoretical analysis of the wing.

All Pertinent wing parameters for each density ratio are tabulated below $b = .855'$

μ	r_α	x_α	a	ω_h/ω_α	ω_α $\frac{rad.}{sec.}$
6.24	.386	.122	-.195	.416	40.6
5.36	.388	.122	-.195	.420	43.4
4.59	.415	.122	-.195	.449	43.9
3.75	.456	.122	-.195	.492	44.3
2.68	.529	.122	-.195	.570	45.2
1.56	.666	.122	-.195	.714	46.9

The Experimental Procedure

Each run was made at a different density ratio. The runs were all identical so one description of the procedure should suffice.

A very rough calculation of each flutter speed was done beforehand in order to allow the experimenter to get a fair idea of the magnitudes of the flutter speeds. The tunnel was switched on and the velocity increased by increments of approximately five miles per hour. Between incremental changes in tunnel speed the wing was excited, to get an idea of the rate of aerodynamic damping of the oscillations. The speed was increased above the flutter speed and the model was held by the excitation chord to prevent damage by large, violent flutter oscillations. The speed was then decreased very slowly until the oscillations were just barely sustained. This was then taken to be the flutter speed.

The runs were made in descending values of density ratio in order to begin with lowest flutter velocities. As the density ratio was changed the static gravity load on the restraints was changed and therefore the zero translational rotational positions were altered for each run. This produced a new equilibrium position (wind on) which often had to be corrected by bending the spring restraints in order to keep the model from hitting the stops during flutter and producing large, non-linear effects.

The flutter speeds ranged from 28 m.p.h. to 62 m.p.h. The last run, made at a density ratio of ($\mu = 1.54$) was probably the most important and also the most dramatic in that it resulted in the destruction of the model. The purpose of this particular run was to increase the tunnel velocity until the model fluttered or was destroyed. The destruction of the model occurred at a tunnel velocity of 62 m.p.h.

All flutter data collected in these tests is represented in Fig. #8.

III

THE THEORY AND THEORETICAL CALCULATIONS

Flutter Analysis

Validation of the typical section analysis, for which the wing was specifically designed obviously necessitates this form of theoretical analysis of the experimental wing. This type of analysis has been thoroughly developed and is the foundation of almost all of the more sophisticated methods of flutter analysis developed to date. A short explanation of this method follows.

The equations of motion of the wing are developed from Lagrange's equation.

$$\frac{d}{dt}\left(\frac{\partial T}{\partial \dot{q}_i}\right) - \frac{\partial T}{\partial q_i} + \frac{\partial U}{\partial q_i} = Q_i \tag{1}$$

After suitable manuipulation of this equation, including the addition of structural damping we obtain

$$m\ddot{h} + S_\alpha \ddot{\alpha} + m[1 + i g_h]\omega_h^2 h = Q_h \tag{2}$$

$$S_\alpha \ddot{h} + I_\alpha \ddot{\alpha} + I_\alpha[1 + i g_\alpha]\omega_\alpha^2 h = Q_\alpha \tag{3}$$

We then specify simple harmonic motion.

$$h = \bar{h}_0 e^{i\omega t} \qquad \alpha = \bar{\alpha}_0 e^{i\omega t}$$

This reduces the equations of motion to

$$-\omega^2 mh - \omega^2 S_\alpha \alpha + \omega_h^2 [1 + ig_h] mh = -L \tag{4}$$

$$-\omega^2 S_\alpha h - \omega^2 I_\alpha \alpha + \omega_\alpha^2 [1 + ig_\alpha] I_\alpha \alpha = M_y \tag{5}$$

Because of the very low flutter speeds involved, incompressible flow is assumed. With familiar methods developed by Theodorsen and Garrick and in the notation of Ref.#2 we obtain

$$L = -\pi\rho b^3 \omega^2 \left\{ L_h \frac{h}{b} + \left[L_\alpha - L_h \left(\tfrac{1}{2} + a \right) \right] \alpha \right\} \tag{6}$$

$$M_y = \pi\rho b^4 \omega^2 \left\{ \left[M_h - L_h \left(\tfrac{1}{2} + a \right) \right] \frac{h}{b} + \left[M_\alpha - (L_\alpha + M_h)\left(\tfrac{1}{2} + a \right) + L_h \left(\tfrac{1}{2} + a \right)^2 \right] \alpha \right\} \tag{7}$$

Substituting equations (6) and (7) into equations (4) and (5) and after appropriate algebraic manipulation we have the dimensionless flutter equations

$$\frac{\bar{h}_0}{b} \left\{ \frac{m}{\pi\rho b^2} \left[1 - \frac{\omega_h^2}{\omega^2} (1 + ig_h) \right] + L_h \right\} + \bar{\alpha}_0 \left\{ x_\alpha \frac{m}{\pi\rho b^2} + \left[L_\alpha - L_h \left(\tfrac{1}{2} + a \right) \right] \right\} = 0 \tag{8}$$

$$\frac{\bar{h}_0}{b} \left\{ x_\alpha \frac{m}{\pi\rho b^2} + \left[\tfrac{1}{2} - L_h \left(\tfrac{1}{2} + a \right) \right] \right\} + \bar{\alpha}_0 \left\{ r_\alpha^2 \frac{m}{\pi\rho b^2} \left[1 - \frac{\omega_\alpha^2}{\omega^2} (1 + ig_\alpha) \right] + M_\alpha - \left(L_\alpha + \tfrac{1}{2} \right)\left(\tfrac{1}{2} + a \right) + L_h \left(\tfrac{1}{2} + a \right)^2 \right\} = 0 \tag{9}$$

From these we obtain the familiar flutter determinant

$$\begin{vmatrix} \left\{\frac{m}{\pi\rho b^2}\left[1-\frac{\omega_h^2}{\omega_\alpha^2}\frac{\omega_\alpha^2}{\omega^2}(1+ig_h)\right]+L_h\right\} & \left\{x_\alpha\frac{m}{\pi\rho b^2}+L_\alpha-L_h\left(\tfrac{1}{2}+a\right)\right\} \\ \left\{x_\alpha\frac{m}{\pi\rho b^2}+\frac{1}{2}-L_h\left(\tfrac{1}{2}+a\right)\right\} & \begin{matrix}\left\{r_\alpha^2\frac{m}{\pi\rho b^2}\left[1-\frac{\omega_\alpha^2}{\omega^2}(1+ig_\alpha)\right]+M_\alpha\right. \\ \left.-\left(L_\alpha+\tfrac{1}{2}\right)\left(\tfrac{1}{2}+a\right)+L_h\left(\tfrac{1}{2}+a\right)^2\right\}\end{matrix} \end{vmatrix}=0$$

To simplify the computations to a reasonable degree we assume

$$g_h=g_\alpha=g$$

We now can write the final flutter determinant.

$$\begin{vmatrix} \left\{\frac{m}{\pi\rho b^2}\left[1-\frac{\omega_h^2}{\omega_\alpha^2}\frac{\omega_\alpha^2}{\omega^2}(1+ig)\right]+L_h\right\} & \left\{x_\alpha\frac{m}{\pi\rho b^2}+L_\alpha-L_h\left(\tfrac{1}{2}+a\right)\right\} \\ \left\{x_\alpha\frac{m}{\pi\rho b^2}+\frac{1}{2}-L_h\left(\tfrac{1}{2}+a\right)\right\} & \begin{matrix}\left\{r_\alpha^2\frac{m}{\pi\rho b^2}\left[1-\frac{\omega_\alpha^2}{\omega^2}(1+ig)\right]+M_\alpha\right. \\ \left.-\left(L_\alpha+\tfrac{1}{2}\right)\left(\tfrac{1}{2}+a\right)+L_h\left(\tfrac{1}{2}+a\right)^2\right\}\end{matrix} \end{vmatrix}=0$$

The determinant was solved by the familiar (V-g) method. Using the wing parameters tabulated at the end of the section entitled <u>Model Parameters and Methods of Obtaining Them</u>, we obtain the curves of Fig.7. Due to the uncertainty of the value of g , we assume that the experimental flutter obtained at the highest density ratio (μ=6.24), coincides exactly with the analytical prediction of flutter at that μ . This is an indirect measure of g which now embodies all of the non-linear, boundary layer, structural damping, and other analytically indeterminant factors which were assumed negligible or emperimentally indeterminant in the initial stages of the analysis. The chosen value is ($g = .075$). This value enables us to draw the theoretical, velocity-density ratio curve depicted in Fig. 8.

Divergence

The divergence speed of the model is calculated from the following equation:

$$U_D = \frac{1}{\sqrt{\frac{\rho}{2} \frac{1}{K_\alpha} S e C_{L_\alpha}}}$$

The calculated divergence speed is ($U_D = 58\text{mph}$). This speed is well above all the experimental speeds except the velocity encountered in the last run ($\mu = 1.54$) which lead to the destruction of the wing. The dimensionless divergence speed encountered for this particular run is indicated on Fig.8. This is then the highest speed and also the highest value of $\frac{U_\infty}{b\omega_\alpha}$ for which flutter was not encountered at this density ratio.

IV.

RESULTS AND DISCUSSION

The experimental results along with the theoretical predictions of flutter are presented graphically in Fig.8. As can be seen from reference to the graph the experimental points were predicted most accurately by the theory. The deviations between theory and experiment are less than ten percent for all of the data points obtained. This is not, however, quite as satisfactory as it might seem at first glance. We must take into account the fact that the damping term g was not experimentally measurable and therefore the curve was fitted to the experimental data gathered at the two highest density ratios. Thus we have an indirect measurement of g as was explained in Section III. In actual practice if the value of g is accurately obtained there should be very good correlation between theory and experiment as can be seen from the curves of Fig.8 where the correct value of g is assumed to have been used in the calculations. This postulate necessitates a change in the definition of g . It is now assumed to be some specific value for any flutterable system embodying all the theoretically indeterminant effects usually assumed negligible.

These effects are usually either analytically indeterminant or quite difficult to measure experimentally. This value will be unique to any particular system and can be inferred, from Fig.8, to be independent of at least the density ratio. The knowledge that this unique value even exists is quite encouraging and opens to the analyst the possibility of accurately calculating flutter speeds in the low density ratio region if the accurate prediction of the value of is possible.

The predicted increase in flutter speed is definitely justified by the experiment. The fact that no flutter was experienced at the lowest density ratio supports this but is not as pertinent as the values of the data points obtained at the two next higher density ratios. These two values indicate a definite increase in the value of the dimensionless flutter speed which implies a sudden increase to infinity of the flutter speed as the density ratio is decreased. This is also supported by the actual experiment as it was performed. When the run at the lowest density ratio($\mu = 1.56$) was made, there seemed to be no tendency for the wing to flutter or for the aerodynamic damping to decrease as the speed increased. As the tunnel speed was increased and the wing excited by the experimenter, the damping increased instead of decreasing as it had in the other tests at higher density ratios. Thus we have definite evidence supporting the aerodynamic theory.

The inconservative estimates of flutter speed encountered in the experiments by the NACA and others, are explained by assuming that the wrong value of g as it was defined above was used in each analysis. This seems to be a reasonable conclusion in view of the close overall fit of the theoretical curve to the data points obtained in this thesis once the correct value of g was assumed. It is believed that correct determination of this system constant would bring the theoretical predictions to close correlation with experimental data.

V.

RECOMMENDATIONS

It is recommended that some work be done to determine whether accurate estimation of the parameter g, as it is defined in this thesis, will actually improve the correlations between theory and experiment in the low μ range. If this is the case there is a good deal of research that might be done in devising ways of accurately predicting correct values of this parameter. The accomplishment of these two goals would eliminate the inaccuracy of theoretical analyses done in this μ range.

VI.

BIBLIOGRAPHY

(1.) Bisplinghoff, R.L., Ashley, H. and Halfman, R.L.; "Aeorelasticity; Addison-Wesley Publishing Co., Inc., Cambridge, Mass. (1955).

(2.) Smilg, B., and Wasserman, L.S., "Application of Three-dimensional Flutter Theory to Aircraft Structures", Air Force Technical Report, 4798, 1942.

(3.) Theodorsen, T., and Garrick, I.E., "Mechanism of Flutter, a Theoretical and Experimental Investigation of the Flutter Problem", N.A.C.A. Report 685, 1940.

(4.) Broadbent, E.G.; The Elementary Theory of Aeroelasticity, Part III--"Flutter of Control Surfaces and Tabs "; Aircraft Engineering, Vol, XXVI, No. 303, May 1954.

(5.) Henry, C.J.; "An Investigation by Analysis and Research of the Flutter Phenomenon in High Speed Hydrofoils"; Thesis, Dept. of Naval Arch. and Marine Engineering, Massachusetts Institute of Technology, June,1957.

(6.) Scanlan, R.H., and Rosenbaum, R., Introduction to the Study of Aircraft Vibration and Flutter; The Macmillan Co., New York, 1951.

(7.) Pratt, R.M.; "An Investigation of the Flutter of Low Density Wings"; Thesis, Dept. of Aero. Engineering, Massachusetts Institute of Technology, Jan., 1952.

(8.) Fung, Y.C.; The Theory of Aeroelasticity; John Wiley & Sons, Inc. New York, 1955.

(9.) Abbott, I.H.; von Doenhoff, A.E., and Stivers, L.C., Jr.; "Summary of Airfoil Data"; N.A.C.A. Technical Report 824, Washington, 1945.

VII.

APPENDICES

Appendix 1

Method for Calculating the Effective Density Ratio of the Experimental Wing

In order to calculate the additional mass contributed by the spring restraints we write the instantaneous kinetic energy equation

$$K.E. = \frac{1}{2}\int_{\text{STRUCTURE}} v^2\, dm \qquad \text{(A-1)}$$

We assume the following spring mode shapes. For the coil springs we have

$$\xi_{C.S.} = h\left(\frac{x}{\ell_{cs}}\right) \qquad \text{(A-2)}$$

and, because the leaf springs are mounted equal distances fore and aft of the elastic axis we can write

$$\xi_{L.S.} = h\left(\frac{\ell_{LS} - x}{\ell_{LS}}\right) \qquad \text{(A-3)}$$

Because of the symmetry of the leaf springs about the elastic axis this mode shape is independent of α . We can now write the instantaneous kinetic energy of the system as

? No α contribution?

$$K.E. = KE_{\text{WING}} + \frac{2}{2}\int_0^{\ell_{cs}} \left\{\dot{h}\left(\frac{x_{cs}}{\ell_{cs}}\right)\right\}^2 dm_{cs} + \frac{4}{2}\int_0^{\ell_{LS}} \left\{\dot{h}\left(\frac{\ell_{LS} - x_{LS}}{\ell_{LS}}\right)\right\}^2 dm_{LS} \qquad \text{(A-4)}$$

$$+ KE_{\substack{\text{SPRING (LS)}\\ \text{ROTATION}}}$$

where

$$KE_{\text{WING}} = \frac{3}{2} m_w (\dot{h})^2 + 3S_\alpha \dot{h}\dot{\alpha} + \frac{3}{2} I_\alpha (\dot{\alpha})^2 \qquad \text{(A-5)}$$

We now make the substitutions

$$dm_{cs} = \rho_s A_{cs}\, dx_{cs}$$

$$dm_{LS} = \rho_s A_{LS}\, dx_{LS}$$

Upon substitution of these terms in equation (A-4) and integration of (A-4) we obtain

$$KE = \frac{3}{2} m_w (\dot{h})^2 + 3 S_\alpha \dot{\alpha} \dot{h} + \frac{3}{2} I_\alpha (\dot{\alpha})^2 + \frac{1}{3} (\dot{h})^2 \ell_{cs} \rho_s A_{cs} + \frac{2}{3} (\dot{h})^2 \ell_{LS} \rho_s A_{LS} + KE_{\substack{\text{SPRING}\\ \text{ROTATION}\\ \text{(LS)}}} \qquad \text{(A-6)}$$

or since

$$\rho_s A \ell = m_s \qquad \text{(A-7)}$$

The kinetic energy equation becomes

$$KE = \frac{3}{2} m_w (\dot{h})^2 + 3 S_\alpha \dot{\alpha} \dot{h} + \frac{3}{2} I_\alpha (\dot{\alpha})^2 + \frac{1}{3} (\dot{h})^2 m_{cs} + \frac{2}{3} (\dot{h})^2 m_{LS} + KE_{\substack{\text{SPRING}\\ \text{ROTATION (LS)}}} \qquad \text{(A-8)}$$

Combining terms in ($\dot{h}^2$) we have

$$KE = \frac{1}{2} \left(3 m_w + \frac{2}{3} m_{cs} + \frac{4}{3} m_{LS}\right) (\dot{h})^2 + 3 S_\alpha \dot{\alpha} \dot{h} + \frac{3}{2} I_\alpha (\dot{\alpha})^2 + KE_{\substack{\text{SPRING (LS)}\\ \text{ROTATION}}} \qquad \text{(A-9)}$$

because

$2m_{cs} =$ total mass of coil springs, M_{cs}

$4m_{LS} =$ total mass of leaf springs, M_{LS}

We can now write the effective mass of the system as

$$M_{EFF.} = \left(3 m_w + \frac{1}{3} M_{cs} + \frac{1}{3} M_{LS}\right) \qquad \text{(A-10)}$$

and therefore

$$\mu_{EFF.} = \mu = \frac{(m_w + \frac{1}{9} M_{cs} + \frac{1}{9} M_{Ls})}{\pi \rho b^2} \qquad \text{(A-11)}$$

This is the density ratio used throughout the analysis.

Appendix 2

Method for Calculating the Rotational and Translational Spring Constants of the Leaf Springs

The leaf springs have uniform properties over their entire length. Bending deformations are assumed to be governed by the Bernoulli-Euler formula

$$M(x) = EI z''(x) \tag{A-12}$$

The deflection of the end of a cantilever beam due to a load applied at that end can be developed from this formula and we have

$$z(\ell) = \frac{\ell^3 P}{3EI} \tag{A-13}$$

The translational spring constant is defined as

$$K_h = \frac{P}{z} \tag{A-14}$$

We have therefore the contribution of the leaf springs as translational restraints

$$K_{h_{LS}} = \frac{3EI}{\ell_{LS}^3} \tag{A-15}$$

Because there are four leaf springs the total spring constant is

$$K_{h_{LS}} = \frac{12\,EI}{\ell_{LS}^3} \tag{A-16}$$

This is then added to the experimentally measured spring constant for the coil springs to obtain the total translational spring constant.

The prediction of the torsional contribution of the leaf springs is slightly more complex. A torsional deflection of the wing will produce both a moment and a force at the cantilever mount. P is the force applied to the spring at the point where it is pinned to the fairing. The moment applied at the point of cantilever is therefore ($M_c = P\ell_{LS}$). Thus we have

$$M_{EA} = Pd + P\ell_{LS} \tag{A-16}$$

The deflection of the point of cantilever of the leaf spring due to a rotational deflection of the wing is

$$z = d \cdot \alpha \tag{A-17}$$

Subsitiution of equations (A-13) and (A-17) into equation (A-16) yields

$$M_{EA} = \frac{3EI\alpha d^2}{\ell_{LS}^3} + \frac{3EI\alpha \ell_{LS} d}{\ell_{LS}^3}$$

The torsional spring constant is defined as

$$K_\alpha = \frac{M_{EA}}{\alpha}$$

The torsional spring constant for each leaf spring is therefore

$$K_\alpha = \frac{3EId^2}{\ell_{LS}^3} + \frac{3EId}{\ell_{LS}^2}$$

And the total torsional spring restraint for the system is

$$K_\alpha = \frac{12EId^2}{\ell_{LS}^3} + \frac{12EId}{\ell_{LS}^2}$$

Appendix 3

Figures 1 through 8

DIAGRAM OF THE EXPERIMENTAL APPARATUS MOUNTED IN THE WIND TUNNEL

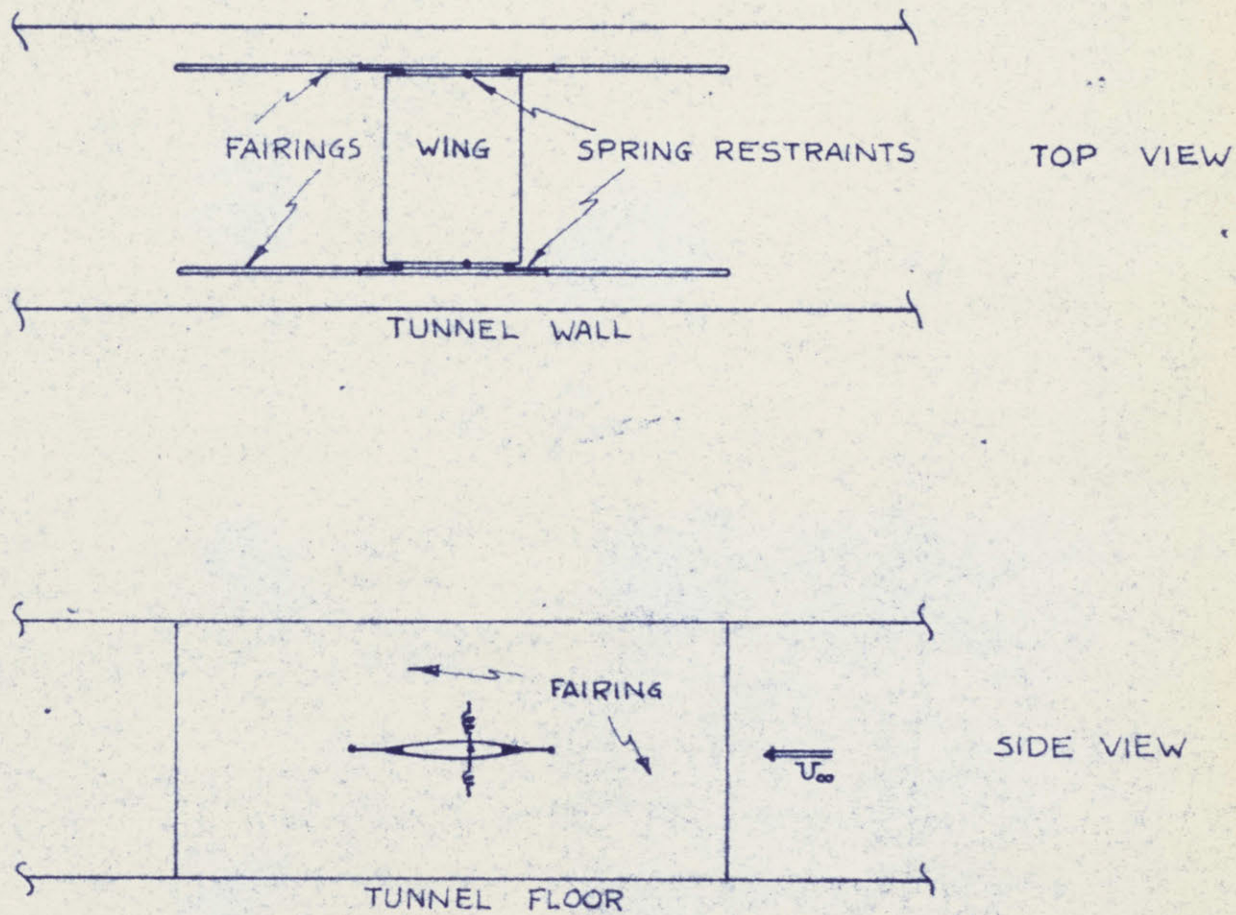

Fig. 1

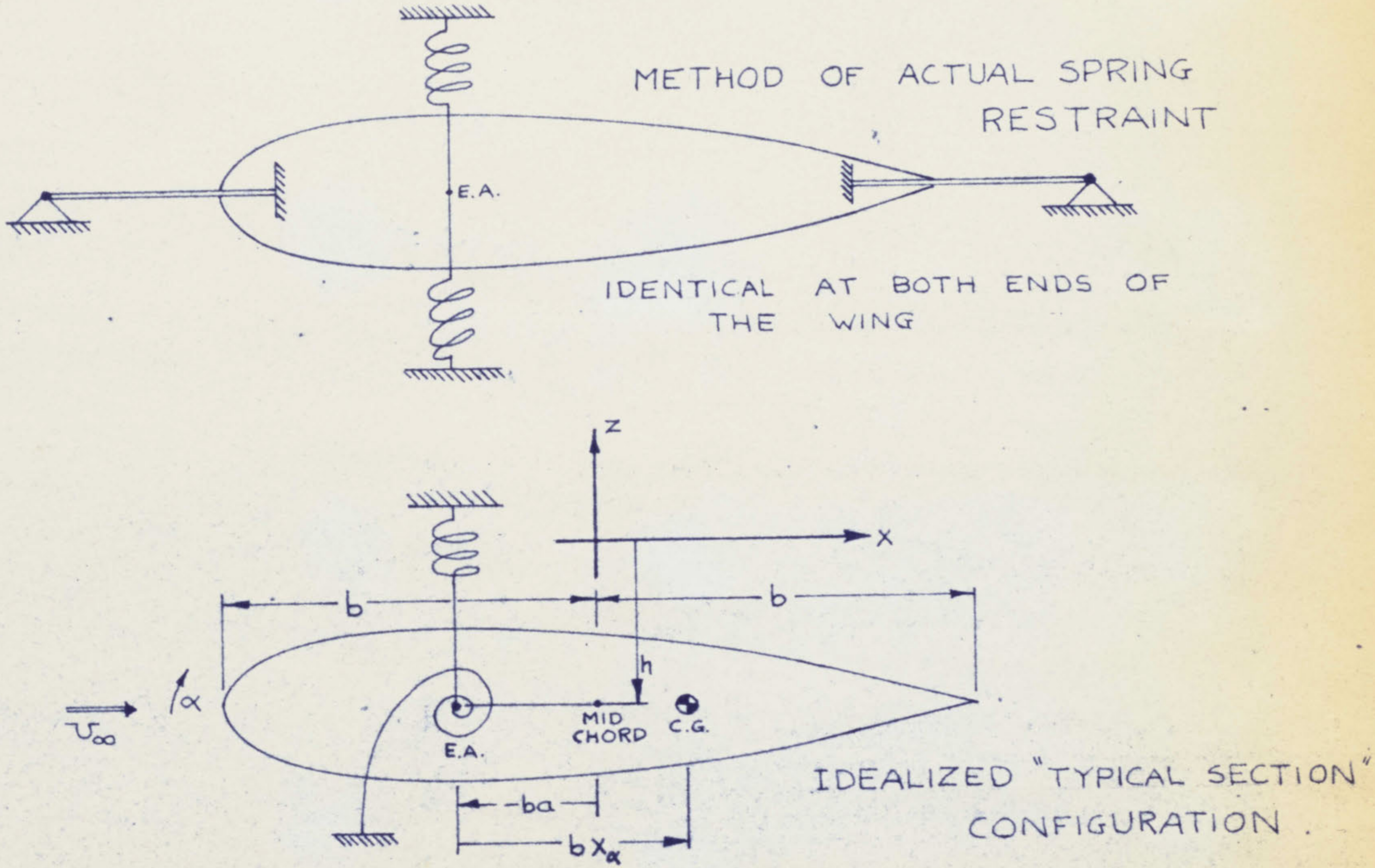
METHOD OF ACTUAL SPRING RESTRAINT
E.A.
IDENTICAL AT BOTH ENDS OF THE WING
z
x
b
b
h
α
v_∞
MID CHORD
C.G.
E.A.
-ba
bx_α
IDEALIZED "TYPICAL SECTION" CONFIGURATION.

Fig. 2

Fig.3 Wing & Fairings Mounted in the Tunnel

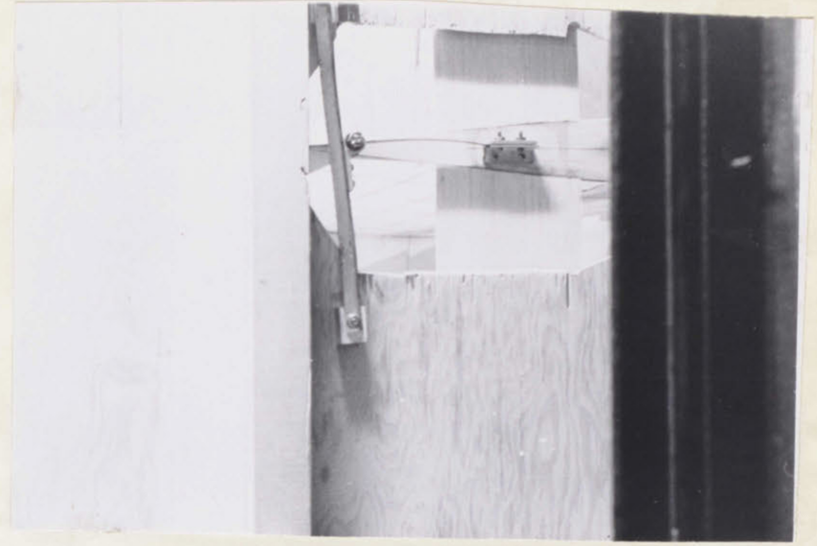

Fig.4 Rear Spring Restraint and its Pin Joint to the Fairing

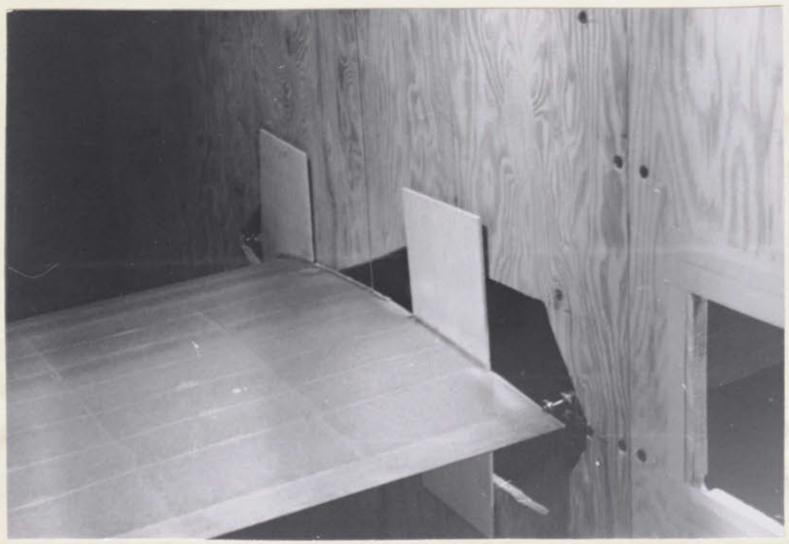

Fig.5 Wing Tip (Fairing Seals Removed)

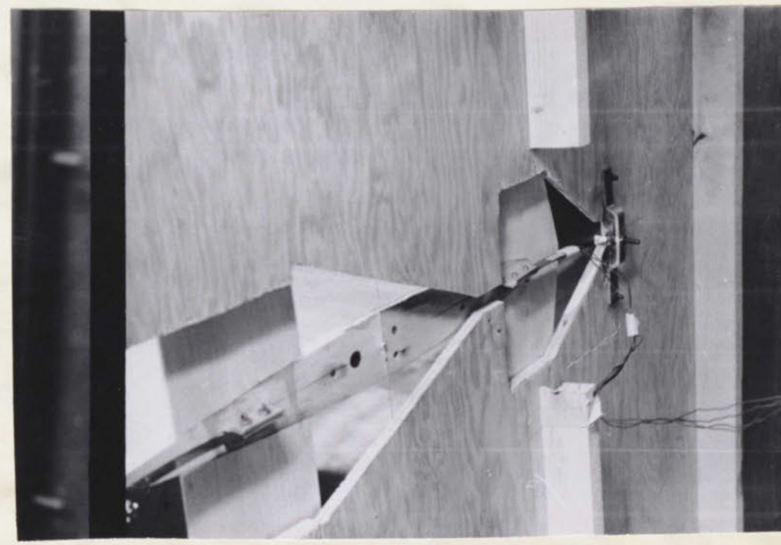

Fig.6 Torsional Spring Restraints

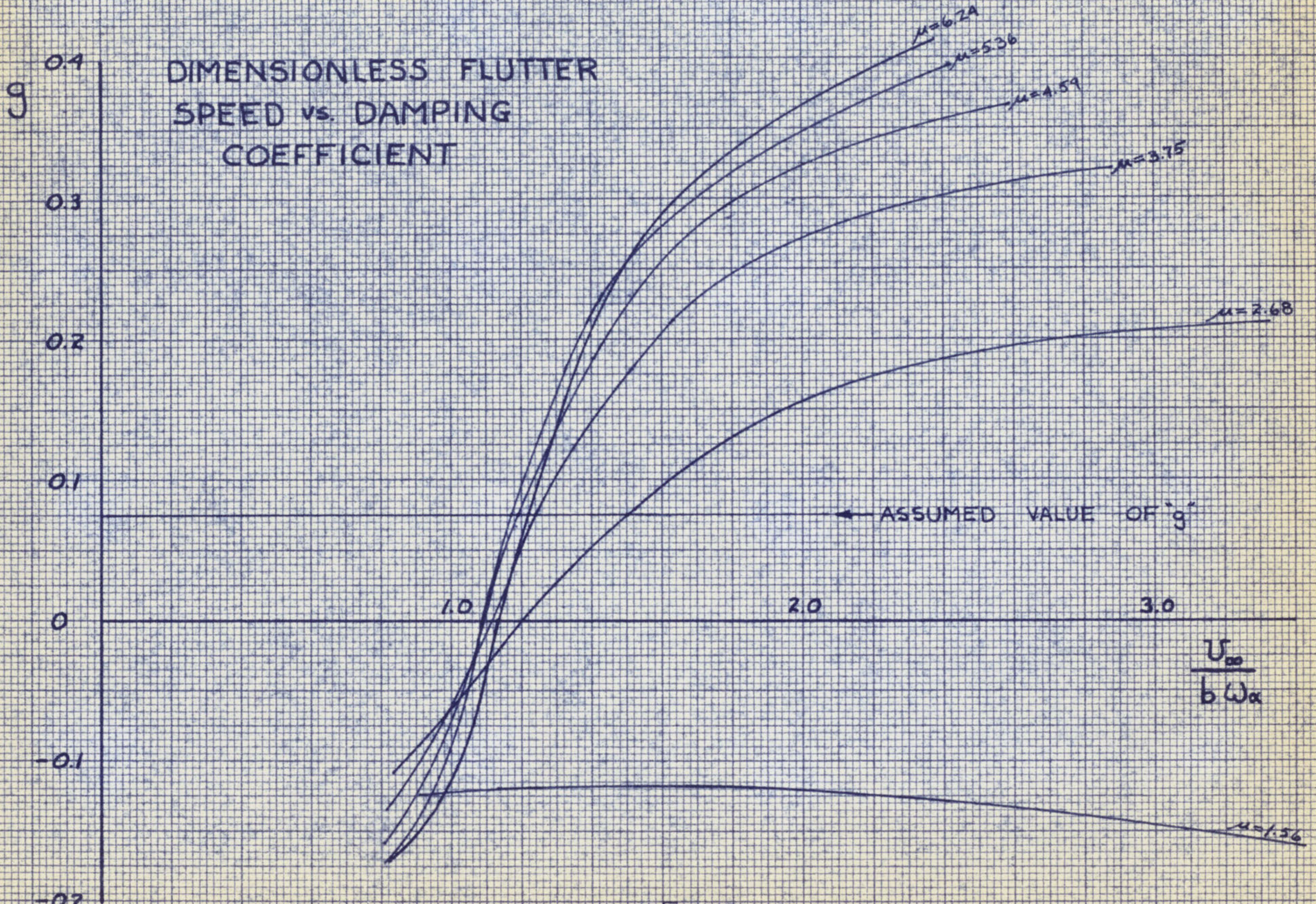
DIMENSIONLESS FLUTTER SPEED vs. DAMPING COEFFICIENT
g
0.4
0.3
0.2
0.1
0
-0.1
-0.2
1.0
2.0
3.0
$\frac{U_\infty}{b\,\omega_\alpha}$
ASSUMED VALUE OF "g"
$\mu=6.24$
$\mu=5.36$
$\mu=4.59$
$\mu=3.75$
$\mu=2.68$
$\mu=1.56$

Fig. 7

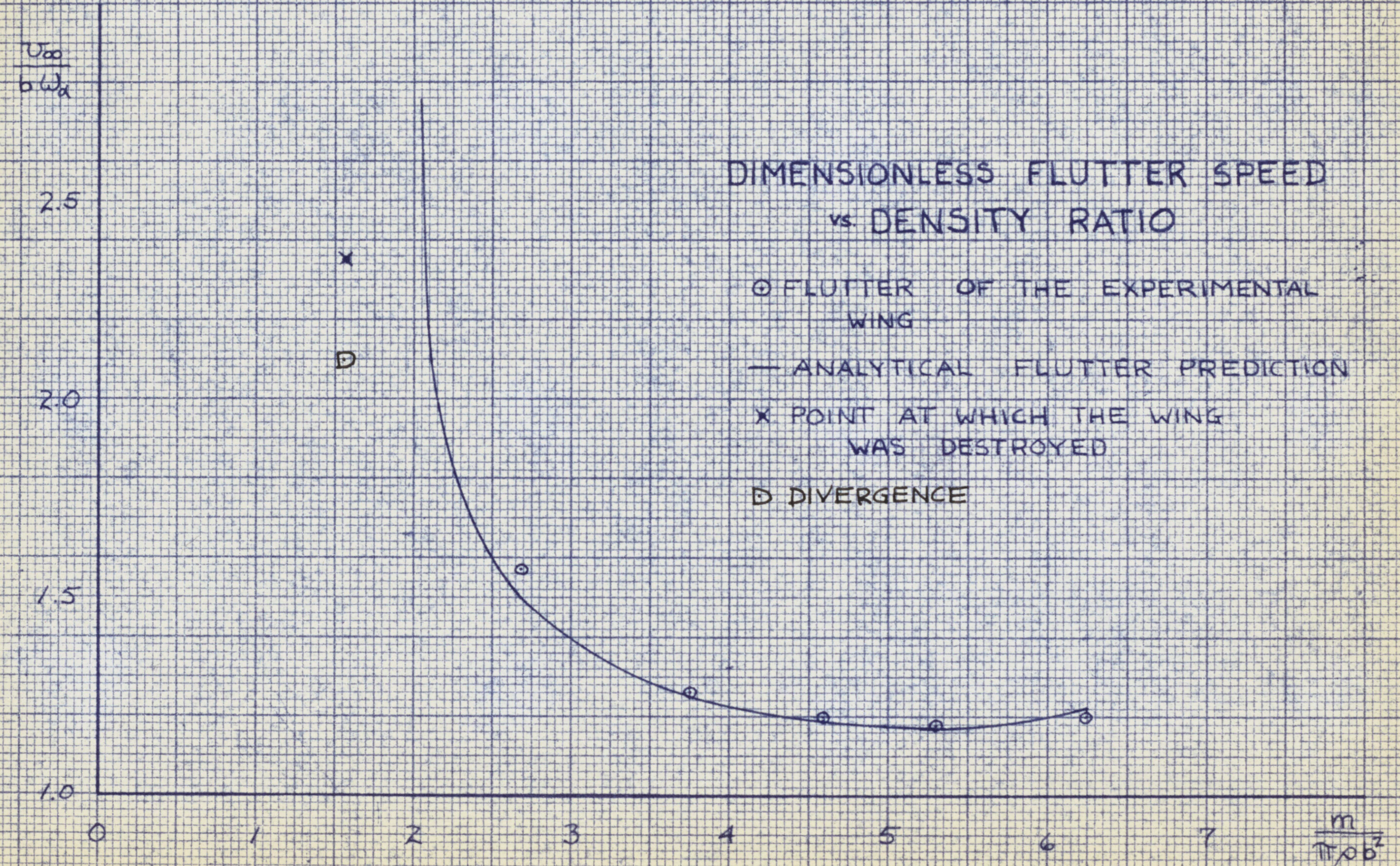

DIMENSIONLESS FLUTTER SPEED
vs. DENSITY RATIO
⊙ FLUTTER OF THE EXPERIMENTAL WING
— ANALYTICAL FLUTTER PREDICTION
× POINT AT WHICH THE WING WAS DESTROYED
D DIVERGENCE
$\frac{U_\infty}{b\omega_\alpha}$
2.5
2.0
1.5
1.0
0
1
2
3
4
5
6
7
$\frac{m}{\pi\rho b^2}$

Fig. 8